Exploring Oscillation Dip and Valley, NSI, and Earth's Core using Atmospheric Neutrinos at INO-ICAL Detector

Based on arXiv:2006.14529, arXiv:2101.02607, arXiv:2104.11740

Anil Kumar

Research Scholar, India-based Neutrino Observatory (INO)

(Institute of Physics, Bhubaneswar, SINP Kolkata, HBNI, Mumbai, India)

Collaborators: Amina Khatun, Sanjib Kumar Agarwalla, Amol Dighe

July 7, 2021

Astroparticle Physics Group Meeting

Department of Physics, University of Alberta

Outline

1. ICAL detector at INO
2. Oscillation Dip and Valley at ICAL
3. Constraining NSI using Oscillation Dip and Valley
4. Validating the Earth's Core using Atmospheric Neutrinos at ICAL

Iron Calorimeter Detector (ICAL) at INO[1]

- **ICAL@INO:** 50 kton magnetized iron calorimeter detector at the proposed India-based Neutrino Observatory (INO)
- **Location:** Bodi West Hills, Theni District, Tamil Nadu, India
- **Aim:** To determine mass ordering and precision measurement of atmospheric oscillation parameters.
- **Source:** Atmospheric neutrinos and antineutrinos in the multi-GeV range of energies over a wide range of baselines.
- **Uniqueness:** Charge identification capability helps to distinguish μ^- and μ^+ and hence, ν_μ and $\bar{\nu}_\mu$
- **Muon energy range:** 1 – 25 GeV, **Muon energy resolution:** $\sim 10\%$
- **Baselines:** 15 – 12000 km, **Muon zenith angle resolution:** $\sim 1^\circ$

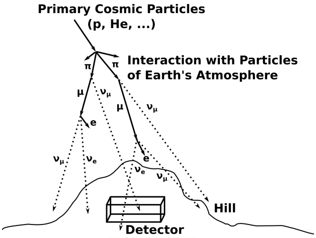

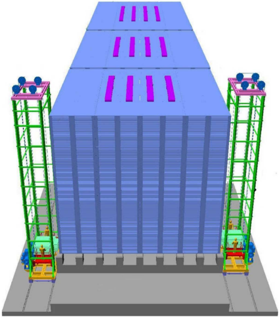

[1] Pramana - J Phys (2017) 88 : 79, arXiv:1505.07380

ICAL Design and Specfications

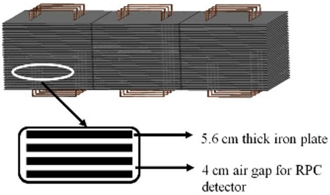

ICAL	
No. of modules	3
Module dimension	16 m × 16 m × 14.5 m
Detector dimension	48 m × 16 m × 14.5 m
No. of layers	151
Iron plate thickness	5.6 cm
Gap for RPC trays	4.0 cm
Magnetic field	1.5 Tesla
RPC	
RPC unit dimension	2 m × 2 m
Readout strip width	3 cm
No. of RPC units/Layer/Module	64
Total no. of RPC units	∼ 30,000
No. of electronic readout channels	3.9×10^6

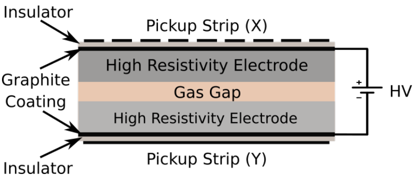

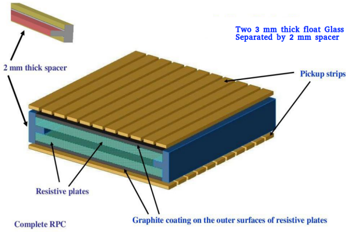

Resistive plate chamber (RPC) (active element) sandwiched between iron plates (passive element)

Pramana - J Phys (2017) 88 : 79, arXiv:1505.07380

Fabrication of RPC

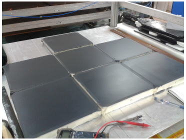

Graphite Coating

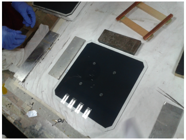

Button Spacers

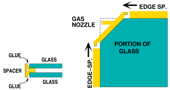

Edge Spacers

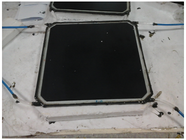

Glued RPC

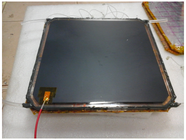

HV Cable Connection

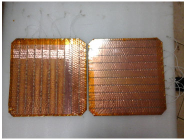

Pick Strip

Packed RPC

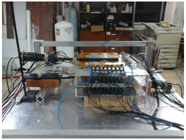

RPC characterization

Note: these photo are taken during course work at INO for fabrication of RPC of size 30 $\times$ 30 cm^2. The actual RPC size at ICAL detector will be 2 $\times$ 2 m^2.

Fabrication of Large Area RPCs

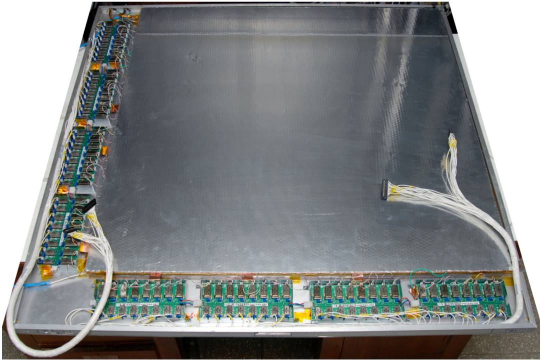

Fully assembled large area glass RPC
(1 m $\times$ 1 m)

http://www.ino.tifr.res.in/ino/

Experimental Modules

2 m $\times$ 2 m Glass RPC stack at TIFR, Mumbai

1 m $\times$ 1 m Glass RPC Stack at TIFR, Mumbai

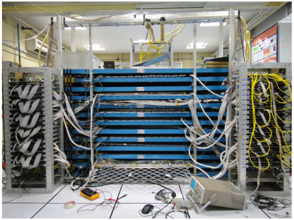

1 m $\times$ 1 m Bakelite RPC Stack with Magnet at VECC, Kolkata

mini-ICAL with Magnet at IICHEP, Madurai

http://www.ino.tifr.res.in/ino/

Detector Response of ICAL

In CC events at ICAL:

- Muon $\rightarrow$ track
- Hadron $\rightarrow$ shower

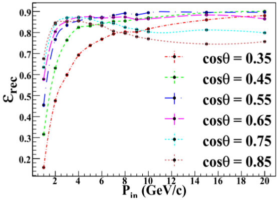

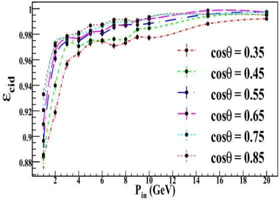

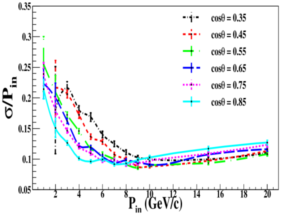

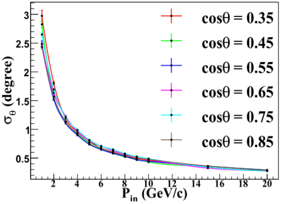

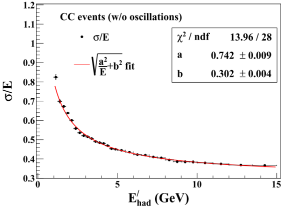

Pramana - J Phys (2017) 88 : 79, arXiv:1505.07380

Neutrino Oscillations in Three-flavor Framework

$$\nu_\alpha = \sum_i U_{\alpha i}\nu_i$$

$$U = \begin{pmatrix} 1 & 0 & 0 \\ 0 & c_{23} & s_{23} \\ 0 & -s_{23} & c_{23} \end{pmatrix} \begin{pmatrix} c_{13} & 0 & s_{13}e^{-i\delta_{\rm CP}} \\ 0 & 1 & 0 \\ -s_{13}e^{i\delta_{\rm CP}} & 0 & c_{13} \end{pmatrix} \begin{pmatrix} c_{12} & s_{12} & 0 \\ -s_{12} & c_{12} & 0 \\ 0 & 0 & 1 \end{pmatrix}$$

where, $c_{ij} = \cos\theta_{ij}$ and $s_{ij} = \sin\theta_{ij}$.

$$P(\nu_\alpha \to \nu_\beta) = \left| U_{\beta 1}U^*_{\alpha 1} + U_{\beta 2}U^*_{\alpha 2}e^{-i2\alpha\Delta} + U_{\beta 3}U^*_{\alpha 3}e^{-i2\Delta} \right|^2$$

$$\text{where,} \quad \Delta m^2_{ij} = m^2_i - m^2_j, \quad \alpha = \frac{\Delta m^2_{21}}{\Delta m^2_{31}} \quad \text{and} \quad \Delta = \frac{\Delta m^2_{31} L}{4E}$$

In this analysis, we use three-flavor oscillation framework in the presence of matter (PREM profile) with the following values of the benchmark oscillation parameters.

$\sin^2 2\theta_{12}$	$\sin^2\theta_{23}$	$\sin^2 2\theta_{13}$	$\lvert\Delta m^2_{32}\rvert$ (eV^2)	Δm^2_{21} (eV^2)	$\delta_{\rm CP}$	Mass Ordering
0.855	0.5	0.0875	2.46×10^{-3}	7.4×10^{-5}	0	Normal (NO)

- Normal Ordering (NO): $(m^2_3 > m^2_2 > m^2_1)$ • Inverted Ordering (IO): $(m^2_2 > m^2_1 > m^2_3)$

$$\Delta m^2_{\rm eff} = \Delta m^2_{31} - \Delta m^2_{21}(\cos^2\theta_{12} - \cos\delta_{\rm CP}\sin\theta_{13}\sin 2\theta_{12}\tan\theta_{23})$$

Oscillation Dip in Muon Neutrino Survival Probability

The L/E dependence of survival probability $P(\nu_\mu \to \nu_\mu)$ in two-flavor oscillation is given as:

$$P(\nu_\mu \to \nu_\mu) = 1 - \sin^2 2\theta_{23} \cdot \sin^2 \left(1.27 \cdot |\Delta m^2_{32}| \left(\text{eV}^2\right) \cdot \frac{L_\nu\,(\text{km})}{E_\nu\,(\text{GeV})}\right)$$

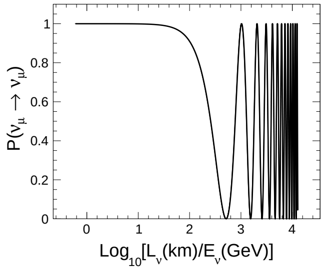

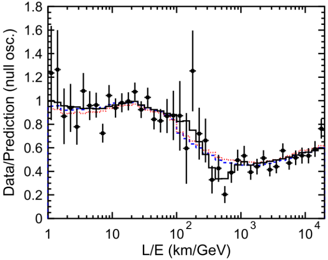

For $\theta_{23} = 45^\circ$ and $\Delta m^2_{32} = 2.4 \times 10^{-3}$ eV^2, $P(\nu_\mu \to \nu_\mu) = 0$ when

$$\frac{1.27 \Delta m^2_{32} L_\nu}{E_\nu} = \frac{\pi}{2}$$

$$\frac{L_\nu}{E_\nu} = 515.35 \text{ km/GeV} \;\&\; \log_{10}\left(\frac{L_\nu}{E_\nu}\right) = 2.71$$

The Super-K experiment was the first experiment to confirm the sinusoidal L/E dependence of the ν_μ survival probability by observing a dip around L/E = 500 km/GeV. (Phys.Rev.Lett. 93 (2004) 101801)

Oscillation Dip and Oscillation Valley in Neutrino

Three-flavor oscillation framework in the presence of matter (PREM profile)

- **Oscillation dip** can be observed around $\log_{10}(L_\nu/E_\nu) = 2.7$
- Matter effect in $P(\nu_\mu \to \nu_\mu)$ for the case of neutrino (due to normal ordering) can be observed around $\log_{10}(L_\nu/E_\nu) = 3.0$
- The **oscillation valley** can be seen as dark blue diagonal band.

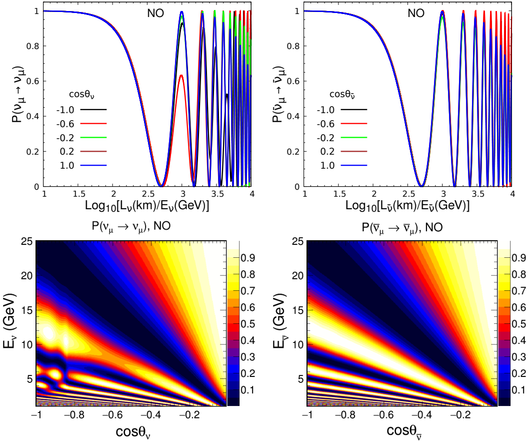

$L_\nu = \sqrt{(R+h)^2 - (R-d)^2 \sin^2\theta_\nu} - (R-d)\cos\theta_\nu$, where R, h, and d are the radius of Earth (6371 km), the average height from the Earth surface at which neutrinos are created (15 km), and the depth of the detector underground (0 km), respectively.

Anil Kumar, Amina Khatun, Sanjib Kumar Agarwalla, Amol Dighe, EPJC 81, 190 (2021), arXiv:2006.14529

Event Generation at ICAL Detector

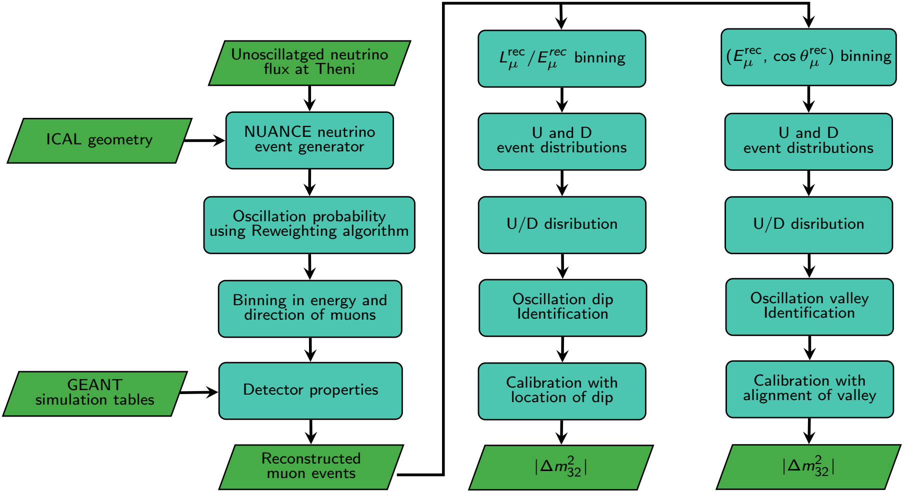

Reconstructed muon events at ICAL

Total number of upward-going (U) and downward-going (D) μ^- and μ^+ events expected at the 50 kt ICAL detector in 10 years (total exposure of 500 kt·yr).

	μ^- events	μ^+ events
U	1654	740
D	2960	1313
Total	4614	2053

U/D ratio (defined for $\cos\theta_\mu^{\text{rec}} < 0$)

$$\text{U/D}(E_\mu^{\text{rec}}, \cos\theta_\mu^{\text{rec}}) \equiv \frac{N(E_\mu^{\text{rec}}, -|\cos\theta_\mu^{\text{rec}}|)}{N(E_\mu^{\text{rec}}, +|\cos\theta_\mu^{\text{rec}}|)} ,$$

where $N(E_\mu^{\text{rec}}, \cos\theta_\mu^{\text{rec}})$ is the number of events with energy E_μ^{rec} and zenith angle θ_μ^{rec}.

Oscillation Dip in Reconstructed Muon Observable at ICAL

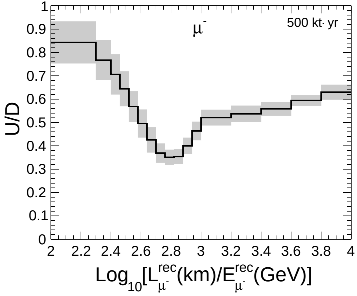

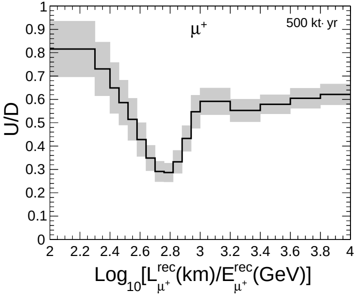

- The light colored boxes show statistical uncertainty calculated using 100 simulated sets of 10-year data.
- The U/D ratio automatically cancels most of the systematic uncertainties.

Anil Kumar et. al. EPJC 81, 190 (2021), arXiv:2006.14529

Identifying the Dip

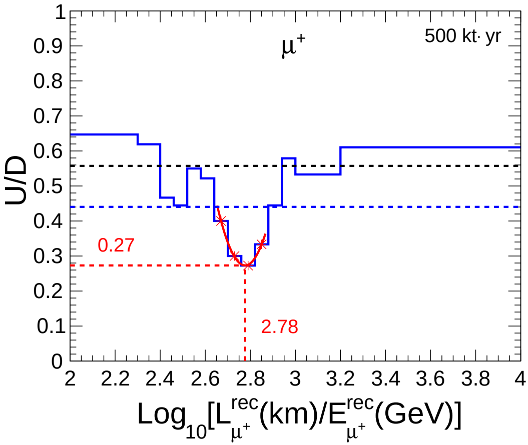

Dip identification algorithm[8] identifies single lowest dip

[8] Anil Kumar et. al. EPJC 81, 190 (2021), arXiv:2006.14529

Estimating Δm^2_{32} using Location of Dip

- We calibrate Δm^2_{32} with respect to the location of dip using 1000 yr MC.
- The 90% C.L. are obtained using multiple simulated sets of 10-year data.

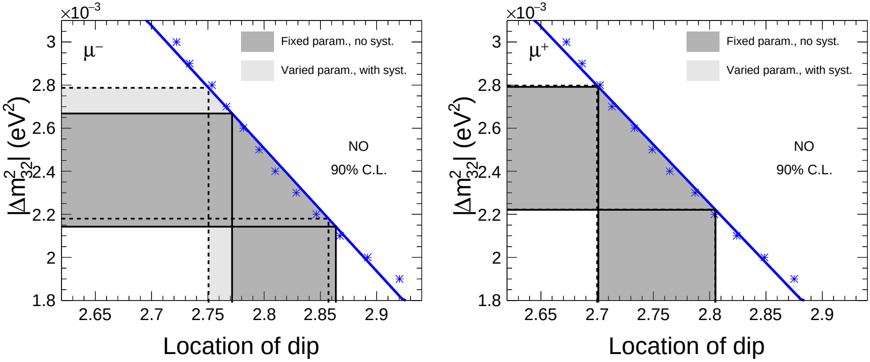

	Δm^2_{32} (in 10^{-3} eV^2) at 90% C.L.	
	μ^-	μ^+
Fixed param., no syst.	2.14 – 2.67	2.22 – 2.79
Varied param., with syst.	2.18 – 2.79	2.22 – 2.80

Anil Kumar et. al. EPJC 81, 190 (2021), arXiv:2006.14529

Oscillation Valley in ($E_\mu^{\rm rec}$, $\cos\theta_\mu^{\rm rec}$) Plane

$$F_0(E_\mu^{\rm rec}, \cos\theta_\mu^{\rm rec}) = Z_0 + N_0 \cos^2\left(m_0 \frac{\cos\theta_\mu^{\rm rec}}{E_\mu^{\rm rec}}\right),$$

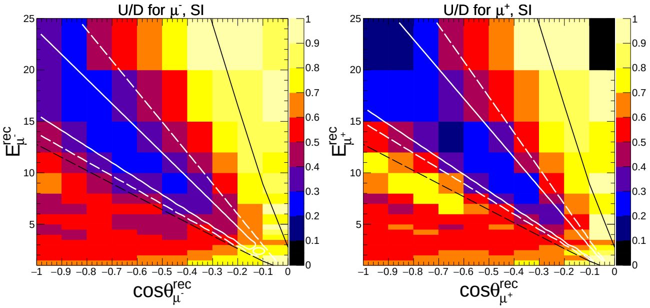

- Mean of 100 U/D distribution for 10 year data.
- Solid black and dashed black lines show conical cut of $\log_{10} L/E = 2.2$ and $\log_{10} L/E = 3.0$ respectively which includes bins used for fitting.
- Solid white and dashed white lines show contours with U/D ratio of 0.4 and 0.5 respectively for fitted function.

Anil Kumar et. al. JHEP 04 (2021) 159, arXiv: 2101.02607

Estimating Δm^2_{32} using Alignment of Oscillation Valley

- We calibrate Δm^2_{32} with respect to m_0 using 1000 yr MC.
- The 90% C.L. are obtained using multiple simulated sets of 10-year data.

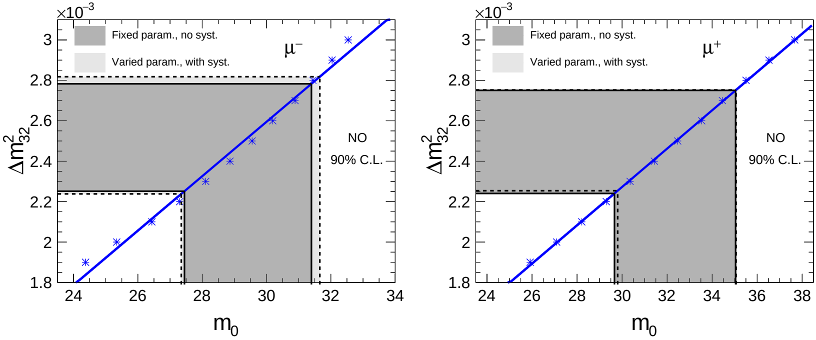

	Δm^2_{32} (in 10^{-3} eV^2) at 90% C.L.	
	μ^-	μ^+
Fixed param., no syst.	2.25 – 2.78	2.24 – 2.75
Varied param., with syst.	2.24 – 2.82	2.25 – 2.75

Anil Kumar et. al. JHEP 04 (2021) 159, arXiv: 2101.02607

Neutral-current Non-Standard Interactions (NSI)

Neutral-current NSI in propagation through matter.

$$\mathcal{L}_{\text{NC-NSI}} = -2\sqrt{2}G_F\varepsilon^{Cf}_{\alpha\beta}(\bar{\nu}_\alpha\gamma^\rho P_L \nu_\beta)(\bar{f}\gamma_\rho P_C f)$$

where, $P_L = (1-\gamma_5)/2, P_R = (1+\gamma_5)/2$, and $C = L, R$.

$$\varepsilon_{\alpha\beta} = \sum_{f=e,u,d} \frac{V_f}{V_{CC}} \left(\varepsilon^{Lf}_{\alpha\beta} + \varepsilon^{Rf}_{\alpha\beta}\right)$$

where, $V_{CC} = \sqrt{2}G_F N_e, V_f = \sqrt{2}G_F N_f, f = e, u, d$.

$$H_{mat} = \sqrt{2}G_F N_e \begin{pmatrix} 1+\varepsilon_{ee} & \varepsilon_{e\mu} & \varepsilon_{e\tau} \\ \varepsilon^*_{e\mu} & \varepsilon_{\mu\mu} & \varepsilon_{\mu\tau} \\ \varepsilon^*_{e\tau} & \varepsilon^*_{\mu\tau} & \varepsilon_{\tau\tau} \end{pmatrix}$$

In atmospheric neutrinos, $\mu-\tau$ channel is dominant, hence, we choose to constrain $\varepsilon_{\mu\tau}$ (only real values)

$$H_{mat} = \sqrt{2}G_F N_e \begin{pmatrix} 1 & 0 & 0 \\ 0 & 0 & \varepsilon_{\mu\tau} \\ 0 & \varepsilon^*_{\mu\tau} & 0 \end{pmatrix}$$

Existing bounds on $\varepsilon_{\mu\tau}$

Experiment	90% C.L. bounds	
	Their Convention ($\tilde{\varepsilon}_{\mu\tau}$)	Our convention[12] ($\varepsilon_{\mu\tau} = 3\,\tilde{\varepsilon}_{\mu\tau}$)
IceCube[13]	$-0.006 < \tilde{\varepsilon}_{\mu\tau} < 0.0054$	$-0.018 < \varepsilon_{\mu\tau} < 0.0162$
DeepCore[14]	$-0.0067 < \tilde{\varepsilon}_{\mu\tau} < 0.0081$	$-0.0201 < \varepsilon_{\mu\tau} < 0.0243$
Super-K[15]	$\lvert\tilde{\varepsilon}_{\mu\tau}\rvert < 0.011$	$\lvert\varepsilon_{\mu\tau}\rvert < 0.033$

Table: Existing bounds on $\varepsilon_{\mu\tau}$ at 90% confidence level. Note that the bounds presented are on $\tilde{\varepsilon}_{\mu\tau}$ that is defined according to the convention $V_{\rm NSI} = \sqrt{2}G_F N_d\,\tilde{\varepsilon}_{\mu\tau}$, while we use the convention $V_{\rm NSI} = \sqrt{2}G_F N_e\,\varepsilon_{\mu\tau}$. Since $N_d \approx 3N_e$ in Earth, the bounds on $\tilde{\varepsilon}_{\mu\tau}$ have been converted to the bounds on $\varepsilon_{\mu\tau}$, using $\varepsilon_{\mu\tau} = 3\,\tilde{\varepsilon}_{\mu\tau}$, as shown in the third column.

[12] Y. Farzan and M. Tortola, Front. in Phys. 6 (2018) 10, arXiv:1710.09360.

[13] J. Salvado, et. al., JHEP 01 (2017) 141, arXiv:1609.03450

[14] IceCube collaboration, Phys. Rev. D 97 (2018) 072009, arXiv:1709.07079

[15] Super-Kamiokande collaboration, Phys. Rev. D 84 (2011) 113008, arXiv:1109.1889

Shift in Dip Location in Reconstructed Muon Observables

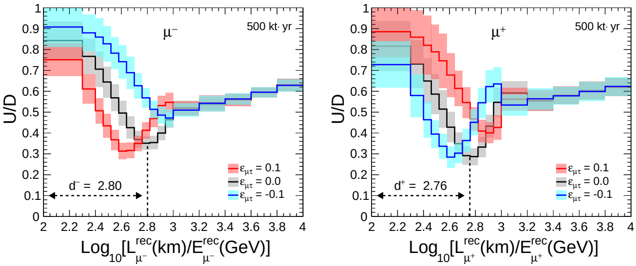

- Statistical uncertainty calculated using 100 simulated sets of 10-year data.
- The location of dip d^- or d^+ depends on magnitude as well as sign of $\varepsilon_{\mu\tau}$.
- d^- and d^+ shift in the opposite direction due to $\varepsilon_{\mu\tau}$.
- d^- and d^+ shift in the same direction due to change in Δm^2_{32}.
- New variable $\Delta d = d^- - d^+$ depends on $\varepsilon_{\mu\tau}$ but independent of Δm^2_{32}(true).

Anil Kumar, Amina Khatun, Sanjib Kumar Agarwalla, Amol Dighe, JHEP 04 (2021) 159, arXiv: 2101.02607

Constraints on $\varepsilon_{\mu\tau}$ from Measurement of Δd

- We calibrate $\varepsilon_{\mu\tau}$ with respect to Δd using 1000 yr Monte Carlo.
- The 90% C.L. are obtained using multiple simulated sets of 10-year data.

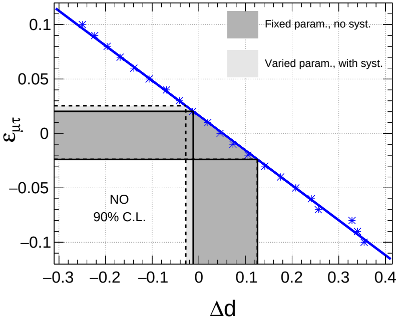

90% C.L.:

- Fixed param., no syst: $-0.024 < \varepsilon_{\mu\tau} < 0.020$
- Varied param., with syst.: $-0.025 < \varepsilon_{\mu\tau} < 0.024$

Anil Kumar et. al. JHEP 04 (2021) 159, arXiv: 2101.02607

Oscillation Valley in Neutrino Survival Probability

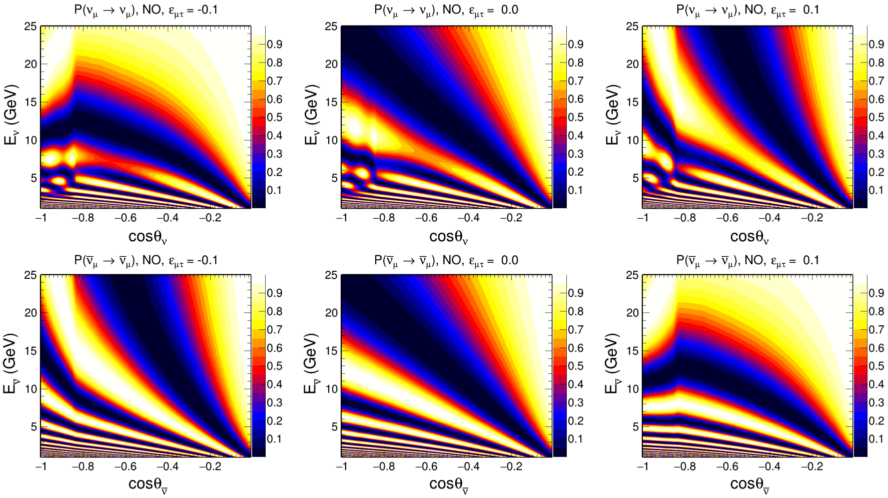

The presence of NSI results in the curvature of oscillation valley (dark blue diagonal band).

Anil Kumar et. al. JHEP 04 (2021) 159, arXiv: 2101.02607

Curvature of Oscillation Valley in Reconstructed Muon Observables

- Mean of 100 U/D distribution for 10 year data in presence of NSI ($\varepsilon_{\mu\tau} = -0.1$ and 0.1).
- Solid black and dashed black lines show conical cut of $\log_{10} L/E = 2.2$ and $\log_{10} L/E = 3.1$ respectively which includes bins used for fitting.
- For $\Delta^2_{21} L/4E \to 0$, $\theta_{13} = 0$, and $\theta_{23} = 45^\circ$ (arXiv:1410.6193), $P(\nu_\mu \to \nu_\mu) = \cos^2\left[L\left(\frac{\Delta m^2_{32}}{4E} + \varepsilon_{\mu\tau} V_{CC}\right)\right]$
- Solid white and dashed white lines show contours with U/D ratio of 0.4 and 0.5 respectively for fitted function $f(x,y) = z_0 + N_0 \cos^2\left(m_\alpha \frac{x}{y} + \alpha x^2\right)$.

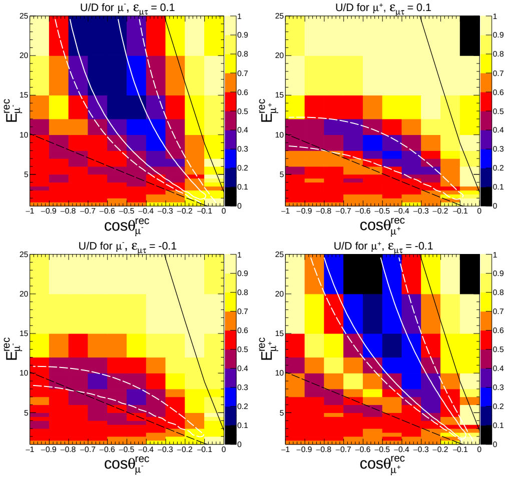

The parameter α is the measure of the curvature of oscillation valley and contains the information about $\varepsilon_{\mu\tau}$.

Anil Kumar et. al. JHEP 04 (2021) 159, arXiv: 2101.02607

Constraints on $\varepsilon_{\mu\tau}$ using Curvature of Oscillation Valley

$\Delta m_\alpha = m_{\alpha^-} - m_{\alpha^+}$ and $\Delta\alpha = \alpha^- - \alpha^+$

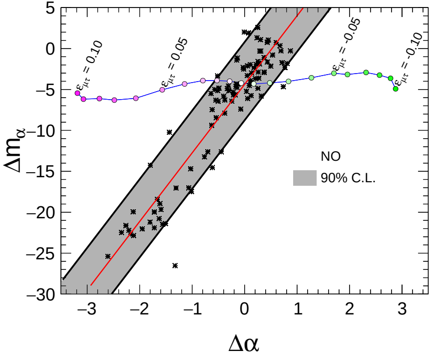

90% C.L.:

- Fixed param., no syst: $-0.022 < \varepsilon_{\mu\tau} < 0.021$
- Varied param., with syst.: $-0.024 < \varepsilon_{\mu\tau} < 0.020$

Anil Kumar et. al. JHEP 04 (2021) 159, arXiv: 2101.02607

Tomography of Earth using Neutrinos

- **Neutrino absorption tomography:** Neutrino attenuation at energies greater than a few TeV. (• Placci, Alfredo and Zavattini, Emilio, 1973, https://cds.cern.ch/record/2258764 • L. Volkova and G. Zatsepin, Izvestiya Akademii Nauk SSSR, Seriya Fizicheskaya 38 (1974), no. 5 1060–1063. • Andrea Donini et. al. Nature Physics volume 15, pages 37–40 (2019))
- **Neutrino oscillation tomography:** The standard W-mediated matter potential V_{CC} experienced by neutrino/antineutrino during interaction with the ambient electrons in the matter can be expressed as

$$V_{CC} = \pm\sqrt{2} G_F N_e \approx \pm 7.6 \times Y_e \times 10^{-14} \left[\frac{\rho}{\mathrm{g/cm^3}}\right] \mathrm{eV}\,, \tag{1}$$

  where, $Y_e = N_e/(N_p + N_n)$ corresponds to the relative electron number density inside the matter and ρ denotes the matter density of various layers inside the Earth for a given profile. The positive (negative) sign is for neutrino (antineutrino). In the present analysis, we assume the Earth to be electrically neutral and isoscalar where $N_n \approx N_p = N_e$ which results in $Y_e = 0.5$.
- **Neutrino diffraction tomography:** The possibility of Earth tomography using the study of diffraction pattern produced by coherent neutrino scattering in crystalline matter inside Earth is technologically not feasible. (A. D. Fortes et. al. Using neutrino diffraction to study the Earth's core, Astronomy and Geophysics 47 (2006), no. 5 5.31–5.33.)

A Brief Review of the Internal Structure of Earth

- Crust: solid, rocks, brittle, lowest density
- Mantle: hot, solid upper mantle, viscous plastic lower mantle
- Core: solid inner core, liquid outer core, iron and nickel

Region	R_{min} (km)	R_{max} (km)	Density (g/cm^3)
Core	0	3480	11.37
Mantle	3480	5701	5
Crust	5701	6371	3.3

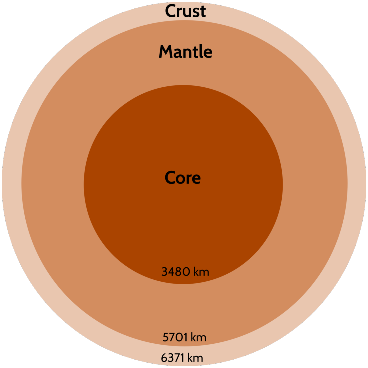

Three-layered model of Earth

References:

E. C. Robertson, The interior of the Earth, an elementary description, 1966.
D. E. Loper and T. Lay, The core-mantle boundary region, Journal of Geophysical Research: Solid Earth 100 (1995), no. B4 6397–6420.
D. Alfè, M. J. Gillan, and G. D. Price, Temperature and composition of the earth's core, Contemporary Physics 48 (2007), no. 2 63–80.

Anil Kumar, Sanjib Kumar Agarwalla, arXiv: 2104.11740

Density Distribution of Various Profiles of Earth

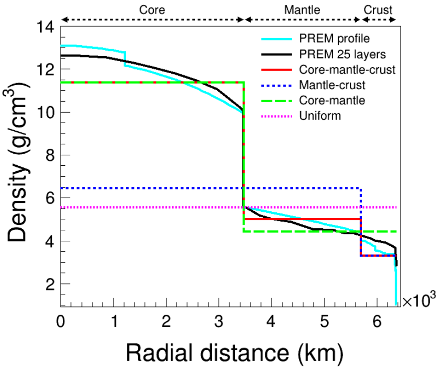

Profiles	Layer boundaries (km)	Layer densities (g/cm^3)
PREM	25 layers	25 densities
Core-mantle-crust	(0, 3480, 5701, 6371)	(11.37, 5, 3.3)
Mantle-crust	(0, 5701, 6371)	(6.45, 3.3)
Core-mantle	(0, 3480, 6371)	(11.37, 4.42)
Uniform	(0, 6371)	(5.55)

Note that while considering alternative profiles of Earth, we assume the radius and the mass of Earth to be invariant.

Anil Kumar et. al. arXiv: 2104.11740

Effect of diff. Density Profiles on $P(\nu_\mu \to \nu_\mu)$ Oscillograms

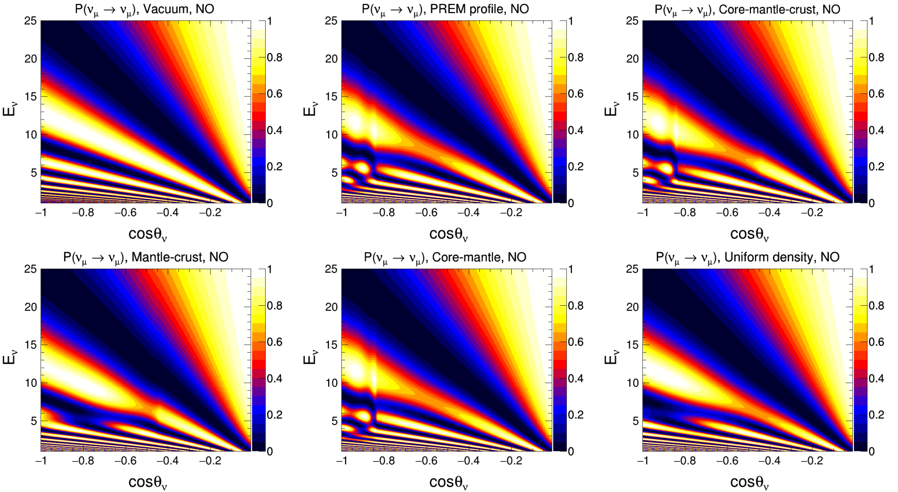

MSW resonance **(L. Wolfenstein, Phys. Rev. D17 (1978) 2369):** red patch around $-0.8 < \cos\theta_\nu < -0.5$ and 6 GeV $< E_\nu <$ 10 GeV

Neutrino oscillation length resonance **(Petcov, Phys. Lett. B 434 (1998) 321)/parametric resonance resonance (Akhmedov, Nucl. Phys. B538 (1999) 25):** yellow patches around $\cos\theta_\nu < -0.8$ and 3 GeV $< E_\nu <$ 6 GeV

Anil Kumar et. al. arXiv: 2104.11740

Effect of diff. Density Profiles on $P(\nu_e \to \nu_\mu)$ Oscillograms

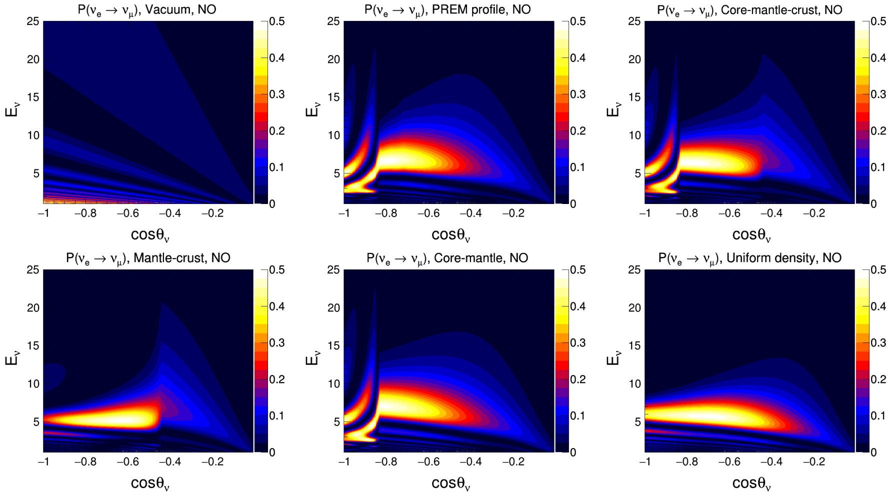

Anil Kumar et. al. arXiv: 2104.11740

Identifying Events for Neutrinos Passing through Different Layers of Earth

- Neutrino flux (Honda) at INO site
- 500 kt·yr exposure at ICAL
- Three-flavor neutrino oscillations in the presence of matter with the PREM profile
- Reconstructed muon events

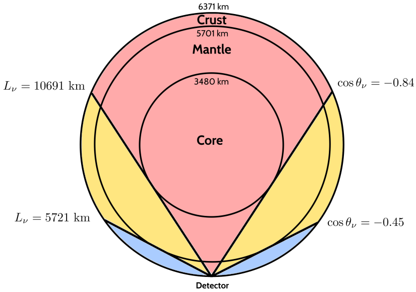

Regions	$\cos\theta_\nu$	L_ν (km)	μ^- Events	μ^+ Events
Crust-mantle-core	(-1.00, -0.84)	(10691, 12757)	331	146
Crust-mantle	(-0.84, -0.45)	(5721, 10691)	739	339
Crust	(-0.45, 0.00)	(437, 5721)	550	244
Downward	(0.00, 1.00)	(15, 437)	2994	1324
Total	(-1.00, 1.00)	(15, 12757)	4614	2053

Anil Kumar et. al. arXiv: 2104.11740

Distribution of Events for Neutrinos Passing through Different Layers of Earth

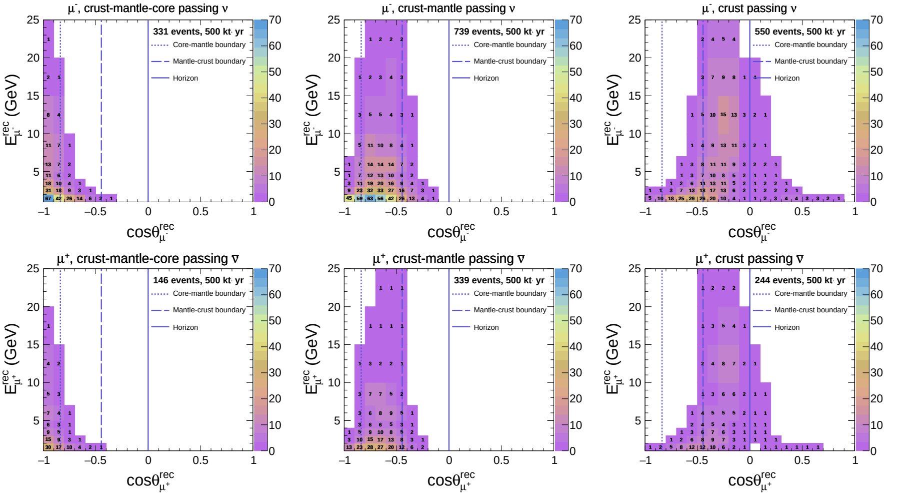

- Neutrino flux at INO site • 500 kt·yr exposure at ICAL • Three-flavor neutrino oscillations in the presence of matter with the PREM profile.

Anil Kumar et. al. arXiv: 2104.11740

Statistical Analysis

In this analysis, the χ^2 statistics is expected to give median sensitivity of the experiment in the frequentist approach.

$$\chi^2_- = \min_{\xi_l} \sum_{i=1}^{N_{E'^{\text{rec}}_{\text{had}}}} \sum_{j=1}^{N_{E^{\text{rec}}_{\mu}}} \sum_{k=1}^{N_{\cos\theta^{\text{rec}}_{\mu}}} \left[2(N^{\text{theory}}_{ijk} - N^{\text{data}}_{ijk}) - 2N^{\text{data}}_{ijk} \ln\left(\frac{N^{\text{theory}}_{ijk}}{N^{\text{data}}_{ijk}}\right)\right] + \sum_{l=1}^{5} \xi_l^2$$

where,

$$N^{\text{theory}}_{ijk} = N^0_{ijk}\left(1 + \sum_{l=1}^{5} \pi^l_{ijk}\xi_l\right)$$

Similarly, χ^2_+ is defined for μ^+

$$\chi^2_{\text{ICAL}} = \chi^2_- + \chi^2_+$$

$$\Delta\chi^2_{\text{ICAL-profile}} = \chi^2_{\text{ICAL}}\ (\text{Mantle-Crust}) - \chi^2_{\text{ICAL}}\ (\text{Core-Mantle-Crust})$$

- Marginalization over systematic uncertainties and $\sin^2\theta_{23}$: (0.36, 0.66), Δm^2_{eff}: (2.1, 2.6) $\times 10^{-3}$ eV^2, and mass ordering: (NO, IO)

Effective Regions in $(E_\mu^{rec}, \cos\theta_\mu^{rec})$ Plane to Validate Earth's Core

• MC Data: Core-mantle-crust • Theory: Mantle-crust • 500 kt·yr exposure at ICAL • Systematic uncertainties are marginalized whereas oscillation parameters are kept fixed in theory

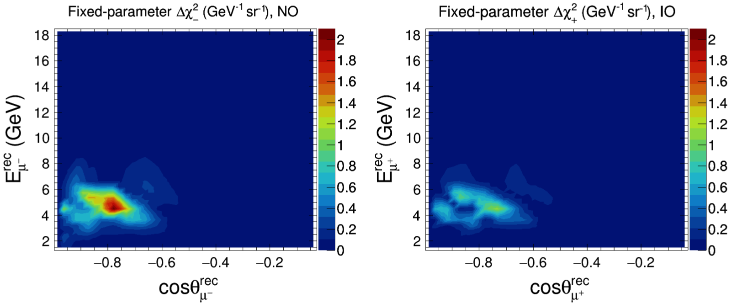

	Fixed-parameter $\Delta\chi^2$	
	NO	IO
Contribution from μ^-	6.85	0.02
Contribution from μ^+	0.05	4.08
Total	6.90	4.10

Note: $\Delta\chi^2_-$ and $\Delta\chi^2_+$ are calculated without pull penalty $\sum_{l=1}^{5}\xi_l^2$ to explore contributions from each bin in $(E_\mu^{rec}, \cos\theta_\mu^{rec})$ plane for μ^- and μ^+ events, respectively.

Anil Kumar et. al. arXiv: 2104.11740

Sensitivity to Validate Earth's Core with and without CID

• 500 kt·yr exposure at ICAL • Marginalization over systematic uncertainties and $\sin^2\theta_{23}$: (0.36, 0.66), $\Delta m^2_{\rm eff}$: (2.1, 2.6) $\times 10^{-3}$ eV^2, and mass ordering: (NO, IO)

MC Data	Theory	$\Delta\chi^2_{\text{ICAL-profile}}$			
		NO(true)		IO(true)	
		with CID	w/o CID	with CID	w/o CID
Core-mantle-crust	Vacuum	4.65	2.96	3.53	1.43
Core-mantle-crust	Mantle-crust	6.31	3.19	3.92	1.29
Core-mantle-crust	Core-mantle	0.73	0.47	0.59	0.21
Core-mantle-crust	Uniform	4.81	2.38	3.12	0.91
PREM profile	Core-mantle-crust	0.36	0.24	0.30	0.11
PREM profile	Vacuum	5.52	3.52	4.09	1.67
PREM profile	Mantle-crust	7.45	3.76	4.83	1.59
PREM profile	Core-mantle	0.27	0.18	0.21	0.07
PREM profile	Uniform	6.10	3.08	3.92	1.18

Anil Kumar et. al. arXiv: 2104.11740

Impact of Marginalization over Various Oscillation Parameters

- 500 kt·yr exposure at ICAL
- Marginalization over systematic uncertainties.
- Marginalization range for $\sin^2\theta_{23}$: (0.36, 0.66), $|\Delta m^2_{\text{eff}}|$: (2.1, 2.6) $\times 10^{-3}$ eV^2, and mass ordering: (NO, IO)

MC Data	Theory	$\Delta\chi^2_{\text{ICAL-profile}}$				
		Fixed parameter	Marginalization over			
			$\sin^2\theta_{23}$	$\lvert\Delta m^2_{\text{eff}}\rvert$	$\pm\lvert\Delta m^2_{\text{eff}}\rvert$	All
Core-mantle-crust	Mantle-crust	6.90	6.36	6.84	6.84	6.31
Core-mantle-crust	Vacuum	6.80	6.44	5.16	4.94	4.65
PREM	Mantle-crust	7.88	7.47	7.81	7.81	7.45
PREM	Vacuum	7.71	7.28	6.10	5.89	5.52

Anil Kumar et. al. arXiv: 2104.11740

Impact of Different True Choices of $\sin^2\theta_{23}$

• 500 kt·yr exposure at ICAL • Marginalization over systematic uncertainties and oscillation parameters $\sin^2\theta_{23}$, $\Delta m^2_{\rm eff}$, and mass ordering.

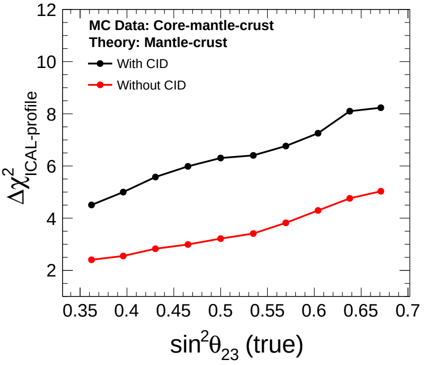

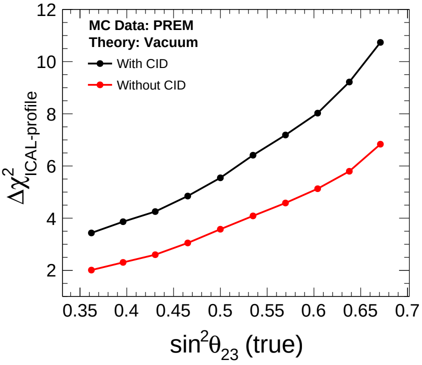

Anil Kumar et. al. arXiv: 2104.11740

Summary and Conclusion

- ICAL has good reconstruction efficiency for μ^- and μ^+ over a multi-GeV range of energies and wide range of baselines.
- Using good energy and directional resolution of ICAL, we demonstrated that the oscillation dip and valley can be observed using the U/D ratio in the reconstructed muon observable.
- The location of dip and alignment of valley were used to estimated 90% C.L. for $|\Delta m^2_{32}|$ for μ^- and μ^+ separately in two different ways.
- We propose a new approach to utilize oscillation dip and oscillation valley to probe neutral-current NSI parameter $\varepsilon_{\mu\tau}$.
- A new variable representing the difference in the shifts in location of dips for μ^- and μ^+ is used to constrain NSI parameter $\varepsilon_{\mu\tau}$.
- The contrasts in curvature of valleys for μ^- and μ^+ is used to constrain NSI parameter $\varepsilon_{\mu\tau}$.
- ICAL can detect 331 μ^- and 146 μ^+ core passing events in 10 years.
- The presence of Earth's core can be independently confirmed at ICAL with a median $\Delta\chi^2$ of 7.45 (4.83) assuming normal (inverted) mass ordering

Acknowledgement

We acknowledge financial support from the Department of Atomic Energy (DAE), Department of Science and Technology (DST), Govt. of India, and the Indian National Science Academy (INSA).

Thank you

Backup: Events and U/D Ratio Using 1000-year MC Simulation

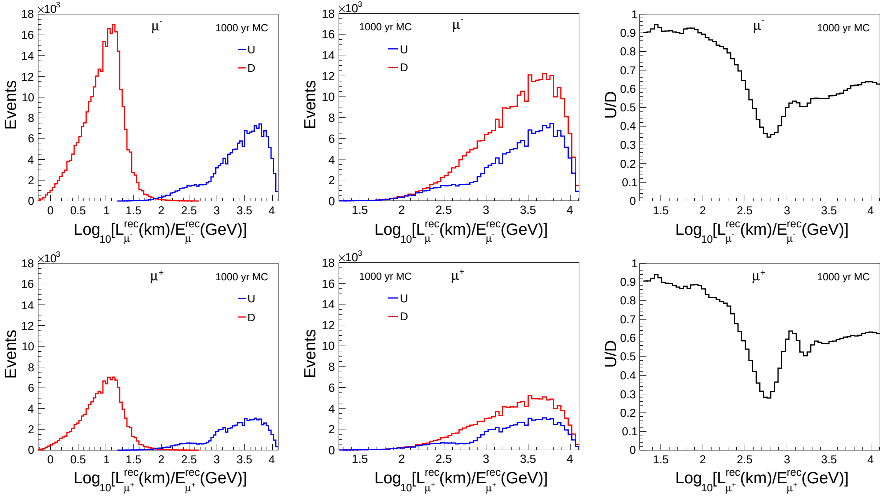

Anil Kumar et. al. EPJC 81, 190 (2021), arXiv:2006.14529

Dip Identification Algorithm

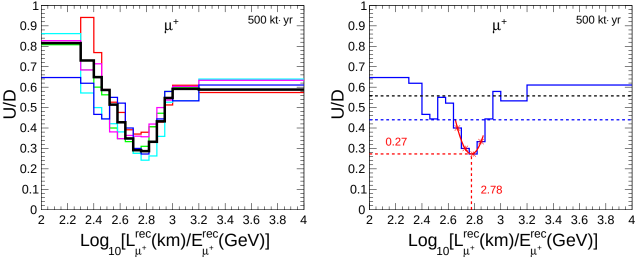

- The left panel shows 5 representative set of 10-year simulated data and thick black line shows mean of 100 simulated sets of 10-year data.
- The right panel shows dip identification algorithm where we start with initial ratio threshold which is shown as dashed black line.
- If ratio threshold passes through more than one oscillation dip then we decrease the ratio threshold.
- The blue dashed line shows the final ratio threshold which passes through only single oscillation dip.
- The bins with U/D ratio less than final ratio threshold are fitted with parabola to obtain location of dip.

Anil Kumar et. al. EPJC 81, 190 (2021), arXiv:2006.14529

Survival probability $P(\nu_\mu \to \nu_\mu)$ in presence of NSI

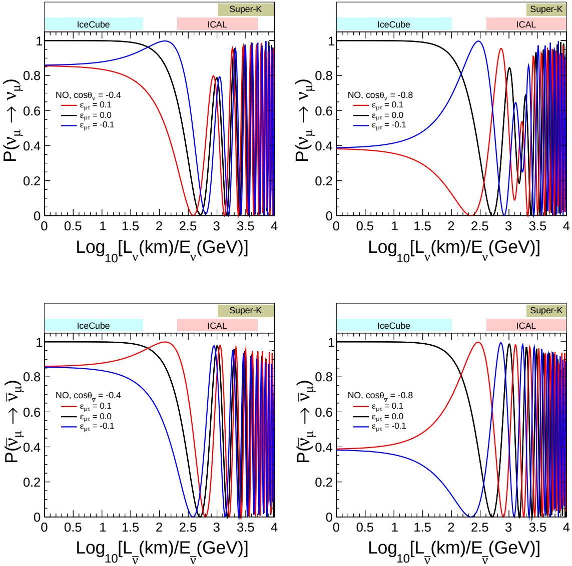

Location of dip shits in the presence of NSI. (Anil Kumar et. al. JHEP 04 (2021) 159, arXiv: 2101.02607)

Backup: Event distribution in presence of NSI

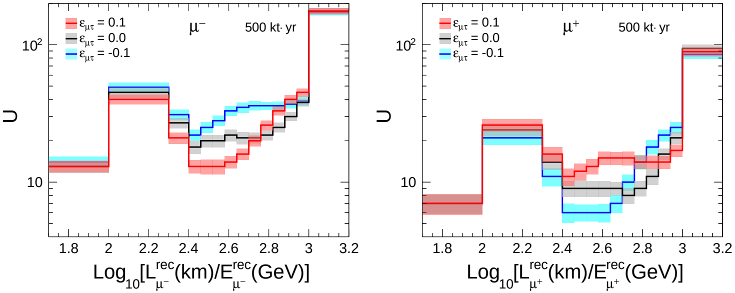

Anil Kumar et. al. JHEP 04 (2021) 159, arXiv: 2101.02607

Backup: Uncertainties in Neutrino Oscillation Parameters

- We first simulated 100 statistically independent unoscillated data sets.
- Then for each of these data sets, we take 20 random choices of oscillation parameters (other than the one going to be measured), according to the gaussian distributions $\Delta m^2_{21} = (7.4 \pm 0.2) \times 10^{-5}$ eV^2 , $\Delta m^2_{32} = (2.46 \pm 0.03) \times 10^{-5}$ eV^2 , $\sin^2 2\theta_{12} = 0.855 \pm 0.020$, $\sin^2 2\theta_{13} = 0.0875 \pm 0.0026$, $\sin^2 \theta_{23} = 0.50 \pm 0.03$, guided by the present global fit.
- We keep $\delta_{\mathrm{CP}} = 0$, since its effect on ν_μ survival probability is known to be highly suppressed in the multi-GeV energy range.
- This procedure effectively enables us to consider the variation of our results over 2000 different combinations of oscillation parameters, to take into account the effect of their uncertainties.

Go Back to slides: Dip valley NSI Dip NSI valley

Anil Kumar et. al. EPJC 81, 190 (2021), arXiv:2006.14529

Backup: Systematic Uncertainties

- The five uncertainties are (i) 20% in overall flux normalization, (ii) 10% in cross sections, (iii) 5% in the energy dependence, (iv) 5% in the zenith angle dependence, and (iii) 5% in overall systematics.
- For each of the 2000 simulated data sets, we modify the number of events in each $(E_\mu^{\rm rec}, \cos\theta_\mu^{\rm rec})$ bin as

$$N = N^{(0)}(1+\delta_1)(1+\delta_2)(E_\mu^{\rm rec}/E_0)^{\delta_3}(1+\delta_4\cos\theta_\mu^{\rm rec})(1+\delta_5)\ ,$$

  where $N^{(0)}$ is the theoretically predicted number of events, and $E_0 = 2$ GeV.
- Here $(\delta_1, \delta_2, \delta_3, \delta_4, \delta_5)$ is an ordered set of random numbers, generated separately for each simulated data set, with the gaussian distributions centred around zero and the 1σ widths given by $(20\%, 10\%, 5\%, 5\%, 5\%)$.

Go Back to slides: Dip Valley Dip NSI Valley NSI

Anil Kumar et. al. EPJC 81, 190 (2021), arXiv:2006.14529

Backup: Reconstructed Events at ICAL using various profiles of Earth

Profiles	Reconstructed μ^- events			Reconstructed μ^+ events		
	Upward	Downward	Total	Upward	Downward	Total
PREM	1654	2960	4614	741	1313	2053
Core-Mantle-Crust	1659	2960	4619	739	1313	2052
Vacuum	1692	2960	4652	745	1313	2057

Anil Kumar et. al. arXiv: 2104.11740